J Therm Anal Calorim (2010) 102:1025–1033
DOI 10.1007/s10973-010-0881-y

Correlations between the morphology and the thermo-mechanical properties in poly(vinyl acetate)/epoxy thermosets

M. Sánchez-Cabezudo · R. M. Masegosa · C. Salom · M. G. Prolongo

Received: 13 November 2009 / Accepted: 11 May 2010 / Published online: 30 May 2010

Abstract The mechanical properties of poly(vinyl acetate) (PVAc)/epoxy thermosets as a function of the PVAc content were investigated through dynamic mechanical thermal analysis from −100 to 220 °C and through tensile tests at room temperature. The morphology of the thermosets was examined by scanning electron microscopy. Cured PVAc/epoxy blends are phase separated, arising two phases that correspond to a PVAc-rich phase and to the epoxy rich-phase. The morphology evolves from nodular to inverted as the PVAc content increases. Intermediate compositions present combined morphologies, in which nodular and inverted regions are detected. The tensile properties at room temperature reveal that combined morphologies present the most ductile behaviour. The glass transition temperatures (T_g) of PVAc and of epoxy phases in the blends are different from those of the neat polymers. The profile of the loss modulus (E'')–temperature curves are correlated with the change in morphology that appears increasing the PVAc content. The storage modulus (E')–temperature curves are highly dependent on the morphology of the samples. The E'-composition dependence is predicted using several models for two-phase composites. The low-temperature β-relaxation of the epoxy is slightly modified by the presence of PVAc. The activation energies of the α and β-relaxations are not dependent on the blend morphology.

Keywords Dynamic mechanical properties · Glass transition · Modulus · Morphology · Tensile test · Thermoplastic–epoxy blends

M. Sánchez-Cabezudo · R. M. Masegosa
Dpt. Física y Química Aplicadas a la Técnica Aeronáutica, E.U.I.T. Aeronáutica Universidad Politécnica de Madrid, Madrid, Spain

C. Salom · M. G. Prolongo (✉)
Dpt. Materiales y Producción Aeroespacial, E.T.S.I. Aeronáuticos Universidad Politécnica de Madrid, Madrid, Spain
e-mail: mg.prolongo@upm.es

Introduction

Highly cross-linked epoxy thermosets are widely used as adhesives and matrices for fibre-composite materials because they possess good combination of thermal and mechanical properties, high glass transition temperature (T_g), stiffness and chemical resistance and low shrinkage on curing. However, they are brittle due to their high crosslink density. Many studies have dealt with the modification of epoxies by adding an elastomeric or a thermoplastic polymer in order to improve their inherent brittleness. The initially miscible blend phase separates on curing to form a biphasic material. In these modified thermosets the morphology, which depends on the modifier content and curing conditions [1], is the main factor that determines the improvement of toughness [2].

Frequently, dynamic mechanical thermal analysis (DMTA) is used to determine the α-relaxation of the phases in modified thermosets. The α-relaxation is related to the segmental dynamics of the polymer chain and is associated to the glass transition temperature (T_g). Most of the systems studied show changes in the position of tan δ, corresponding to the α-relaxations of the phases, which are attributed to a partial miscibility of the components either to an incorrect formation of the epoxy network [3–7]. Some works also study the activation energies of the relaxations

relating them with the interactions [7, 8]; however, the variation of the loss modulus and the prediction of the storage modulus using models is rarely reported [4, 9]. Epoxy networks also present a secondary β-relaxation which is related to local dynamics of hydroxypropylether units [10]. In rubber-modified epoxies, the epoxy β-relaxation appears in the same region of the rubber α-relaxation thus being difficult to differentiate them [3], on the other hand few works have studied the epoxy β-relaxation in thermoplastic/epoxy thermosets [7]. Moreover, they do not often make a joint discussion of the dynamic mechanical and tensile test properties, their prediction by mechanical models and correlation with the morphology.

Poly(vinyl acetate) (PVAc) is an amorphous polymer that features excellent adhesion to various substrates, and is mainly produced for its use in adhesives and paints. The T_g of PVAc is slightly higher than room temperature ($\sim$44 °C), it behaves brittle and rigid at $T < T_g$, but blending with other polymers frequently improves mechanical properties [11].

In previous works [12–15], we have studied the curing of epoxy resins based on diglycidyl ether of bisphenol A (DGEBA) blended with PVAc, using aromatic diamines as curing agents. The initial mixture consists of a thermoplastic dissolved in the epoxy resin precursor (epoxy monomer + curing agent). On curing, the blends phase separate, giving rise to biphasic material formed by an epoxy rich phase and a PVAc rich phase, cured blends show changes in morphology as the PVAc content increases. On the other hand, it has been reported that epoxy thermosets modified with PVAc of high-molecular-weight have higher fracture toughness than neat epoxy thermosets [16]. In this work, we study the dynamic-mechanical properties of DGEBA + PVAc blends cured with 4,4′diaminodiphenylmethane (DDM) in the composition range 5–25 wt% of PVAc, from −100 to 220 °C. Tensile tests of the thermosets were also investigated at room temperature. In PVAc/epoxy thermosets, the epoxy β-relaxation does not overlap with PVAc relaxations thus the effect of morphology on the secondary relaxation could be clearly studied. The aim of this study is to analyse the influence of the PVAc content on the thermo-mechanical behaviour, to correlate it with the sample morphology and to study the predictions of mechanical models.

Experimental

Materials and blend preparation

The epoxy resin was based on the DGEBA manufactured by Ciba under the commercial name of Araldit F. The number average relative molecular mass, $\bar{M}_n = 360$ g mol^{-1}, was obtained by chemical titration of the end groups. The curing agent, DDM (97 wt% purity), was supplied by Across Organics. PVAc with $\bar{M}_n = 9 \times 10^4$ g mol^{-1} and polydispersity index 2 was purchased from Polysciences. Frekote from Loctite was employed as a mould-release product.

DGEBA and DDM were used with a stoichiometric ratio amino-hydrogen to epoxy. (DGEBA + DDM)/PVAc blends were obtained solving appropriate amounts of PVAc in the epoxy resin at 90 °C, then pulverized DDM was solved during 3 min, at this stage all the mixtures were transparent, thus indicating miscibility. To prepare specimens for DMTA, scanning electron microscopy (SEM) and tensile tests measurements, the mixtures were poured into pre-heated moulds at 120 °C, degassed for 6 min and cured under atmospheric pressure. The curing protocol was 120 °C for 2 h and post-curing of 1 h at 180 °C. After curing, the mould was allowed to cool gradually to room temperature. This protocol conduces to totally cured samples. The PVAc content ranged from 5 to 25 wt%.

Techniques

DMTA was performed in dual cantilever bending mode using a DMTA V Rheometric Scientific instrument. Specimens had dimensions: 35 mm × 10 mm × 1.5 mm. The measurements were done at 1, 2, 6, 10, 40 and 50 Hz frequency, with temperature increasing from 30 to 220 °C (high-temperature scan) and from −100 to 30 °C (low-temperature scan) at a heating rate of 1 °C min^{-1}. The maxima on tan δ-temperature curves were determined to identify the α-relaxations associated to the glass transitions and the β-relaxation of the epoxy thermoset.

A Mettler Toledo mod.822e differential scanning calorimeter (DSC) was used to measure the glass transition temperatures and to asses the full cure of the thermosets. Measurements were done at a heating rate of 10 °C min^{-1}, under nitrogen atmosphere. The instrument was calibrated with indium and zinc. Samples of 10–20 mg were used.

SEM was used to study the morphology. A Phillips XL30 instrument was employed with beam energy of 20 kV. The fracture surfaces of the samples were coated with gold by vapour deposition using a vacuum sputter. The environmental mode (ESEM) was also used, with water vapour pressure 0.6–0.7 Torr.

The tensile properties (tensile modulus, tensile strength and elongation at break) were measured on a MTS QTest/2L mechanical tester, with a load cell of 10 kN, using a crosshead speed of 1 mm min^{-1} at room temperature (20–22 °C). The extensometer used was MTS model 634.11F-54 (gauge length 25 mm). The tensile specimens had dimensions: 140 mm × 10 mm × 1.8 mm. Seven specimens for each blend composition were prepared.

Results and discussion

Morphological analysis

Figures 1, 2 and 3 show the micrographs of the fracture surfaces. Neat epoxy (Fig. 1a) presents homogeneous morphology with no visible phase domains; however, the fracture surfaces of the modified epoxies (Figs. 1c, 2b, d and 3) show two different phases, this heterogeneous morphology agrees with the opacity observed in these samples. In the sample with 5 wt% PVAc nodular morphology is observed (Fig. 1c), in which the thermoplastic phase is homogeneously dispersed as small spheres (~0.1 μm in diameter) in a continuous epoxy matrix. However, samples containing 10 and 15 wt% PVAc (Fig. 2b, d) present a combined morphology of nodular morphology regions and inverted morphology regions in which the epoxy phase forms spheres that are surrounded by the thermoplastic phase. When the PVAc content increases up to 20 wt% the morphology changes to totally inverted, showing a packing of epoxy spheres

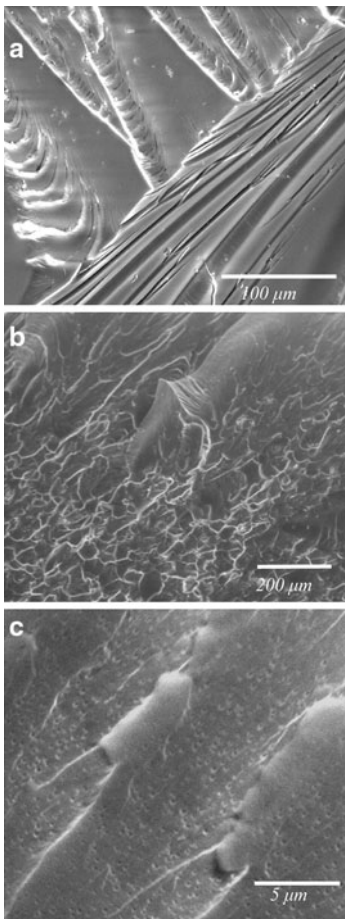

Fig. 1 ESEM micrographs of neat epoxy thermoset at magnification: **a** ×350, and of 5 wt% PVAc/epoxy thermoset at magnifications: **b** ×100 and **c** ×5000

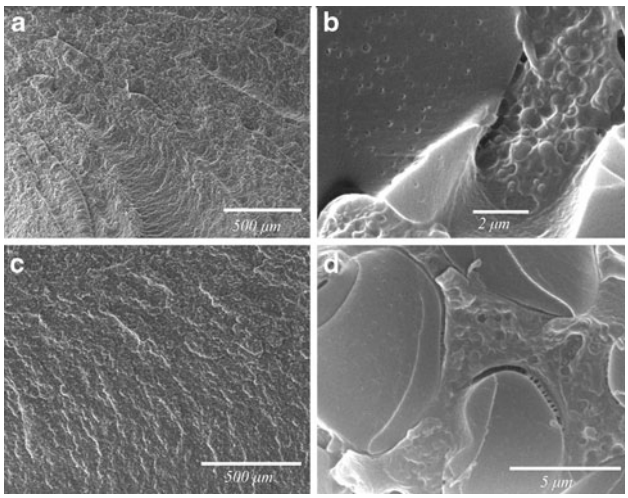

Fig. 2 SEM micrographs of 10 wt% PVAc/epoxy thermoset at magnifications: **a** ×50 and **b** ×10000, and of 15 wt% PVAc/epoxy thermoset at magnifications: **c** ×50 and **d** ×5000

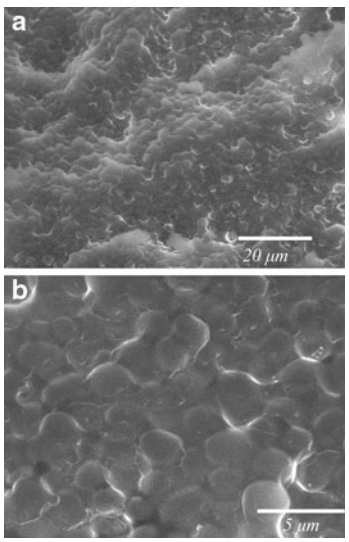

Fig. 3 ESEM micrographs of 20 wt% PVAc/epoxy thermoset at magnifications: **a** ×1000 and **b** ×5000

(~0.8–1.2 μm in diameter) surrounded by a thin continuous PVAc phase (Fig. 3).

The composition at which inversion in morphology takes place should be close to the critical point ϕ^{c}. The thermodynamic description [1] based on the Flory–Huggins model that takes into account the thermoplastic polydispersity was used to calculate the critical composition, using the relation

$$\phi_{TP}^{c-1} = 1 + \left[\frac{V_{TP}}{V_{TS}}\right]^{1/2} \frac{x_w(TP)}{x_z(TP)^{1/2}} \quad (1)$$

where ϕ_{TP}^{c} is the volume fraction of the thermoplastic (PVAc) at the critical point, V_{TP} is the molar volume of the repeating unit of the thermoplastic and V_{TS} is the molar

volume of the thermoset precursor which is taken as a single pseudomonomer (2/3 mol DGEBA and 1/3 mol DDM), and x_w(TP) and x_z(TP) are the degrees of polymerization of the thermoplastic. The molar volumes were obtained from the densities and the polymerization degrees from GPC. The value obtained for the critical composition was $\phi^c_{PVAc} = 0.052$ (~5 wt% PVAc). The morphological study indicated that this composition is not inverted and that the inversion in morphology has already started in blends with 10 wt% PVAc. These differences can be attributed to the interactions between PVAc and epoxy [12] that are not considered in the combinatorial model (Eq. 1).

In samples having compositions near to ϕ^c a variety of morphologies may be developed [1]. The origin of the combined morphology would be a primary phase separation epoxy-rich phase and thermoplastic-rich phase, followed by a secondary phase separation occurring in both phases [17]. This combined morphology was also observed in samples cured after casting from acetone solutions [14]. However, when a much higher molecular weight of PVAc (6.7×10^6 g mol^{-1}) is used, samples with 10 and 15 wt% PVAc show co-continuous morphologies, but the second phase separation was not detected [16].

As it was expected, the fracture surface of neat epoxy (Fig. 1a) is smooth. The smoothness of the fracture surface is typical of the brittle fracture of high T_g epoxy thermosets. The fracture surfaces for PVAc/epoxy samples (Figs. 1b, 2a, c), present tortuous ridges and river marks, the rough fracture surface indicates deflection of crack path hence a higher energy is required for its propagation. This behaviour agrees with the improvement of toughness reported for high-molecular-weight PVAc/modified epoxy [16] and with our tensile tests (see below).

In the nodular morphology regions (Figs. 1c, 2b, 2d) holes can be observed, in which the PVAc particles are missing thus pointing out that they have debonded from the matrix during fracture. In combined morphologies, nodular and inverted regions are intertwined; these regions appear partially debonded on the fracture surfaces, although fibrils connecting the interfaces maintain linked both regions (Fig. 2d). This indicates that there is a significant interpenetration of PVAc and epoxy at the interfaces, which is supported by the fact that none of these samples were disintegrated when they were immersed in good solvents for PVAc. Moreover, for inverted morphologies (Fig. 3) the fracture proceeds without debonding of epoxy particles that are still covered by the thermoplastic layer, thus PVAc matrix determines the failure.

Tensile tests

The stress–elongation curves of neat epoxy thermoset and modified epoxy thermosets with different PVAc content were measured at room temperature (20–22 °C). From the curves the elastic modulus, the tensile strength and the elongation at break were determined, the mean values taken from an average of at least six specimens are given in Table 1. Neat epoxy thermoset and neat PVAc are at room temperature in the glassy state, thus both behave rigid, PVAc is weaker and more fragile than epoxy thermoset. As can be seen for samples with nodular and combined morphologies (5–15 wt% PVAc), Young's modulus changes very little, the tensile strength decreases and the elongation at break increases with increasing the PVAc content, therefore the modified PVAc/epoxy thermosets exhibit a ductile behaviour especially for combined morphologies. The increase in the elongation at break is usually taken as an indication of good adhesion between phases [18], which agrees with the fibrils observed on the fracture surfaces of samples with combined morphology. The area under the stress–strain curves, which is a measure of toughness, was calculated, the results are summarized in Table 1, higher values of the area were obtained for combined morphologies. This behaviour is well correlated with the improvement of toughness reported for high-molecular-weight PVAc/epoxy thermosets [16], the fracture toughness (K_{Ic}) results are listed in Table 1. For co-continuous (combined) morphologies a decrease in toughness is frequently observed when the thermoplastic content increases [2], this has been associated to poor interfacial bonding. Nevertheless in PVAc/epoxy thermosets the samples with combined morphology show the highest toughness in accordance with good interfacial interactions. For samples with inverted morphology (20 wt% PVAc) the behaviour drastically changes, modulus increases, but the tensile strength and the elongation at break, decrease significantly. This is a consequence of the morphology, the PVAc forms the continuous phase (Fig. 3), the fracture occurs through the PVAc matrix which is the weakest phase and it determines the fracture properties.

Table 1 Tensile modulus, tensile strength, elongation at break and area under the tensile curve at room temperature (20–22 °C) and fracture toughness, K_{Ic}, for neat epoxy and for PVAc/epoxy thermosets with different contents of PVAc

PVAc/ wt%	Young's modulus/ GPa	Tensile strength/ MPa	Elongation at break/%	Area/ MJ m^{-3}	K^a_{Ic}/ MPa m$^{1/2}$
0	2.5	63	3.8	135	1.07
5	2.4	62	4.4	163	1.2
10	2.2	59	5.9	228	1.35
15	2.3	52	6.7	274	1.4
20	3.0	36	1.5	27	–
100	3.7	35	1.3	27	–

[a] Data from ref. [16]

Dynamic mechanical thermal analysis

Figure 4 shows the tan δ-temperature isochrones from 30 to 220 °C for samples containing 5, 10, 15 and 20 wt% PVAc. It can be seen that the blends exhibit two α-relaxation peaks which are related to the glass transition of the epoxy network and of the PVAc. The tan δ peaks located at ~38–52 °C correspond to the α-relaxation of PVAc phase and the tan δ peaks located at ~167–175 °C correspond to the α-relaxation of the epoxy network. These values are close to the ones corresponding to the neat polymers; hence, suggesting a high extent of phase separation. The tan δ peak temperatures are reported in Table 2 together with the T_g values obtained from DSC, as usual T_g values by DSC are a few degrees lower than those obtained from the maxima in tan δ at 1 Hz [19].

For blends having 20 and 25 wt% PVAc, which present inverted morphology, the temperature of PVAc tan δ peak coincides with the one of pure PVAc (52 °C), indicating that PVAc phase in this morphology is practically a neat phase. However, in the samples with nodular and combined morphologies (5, 10 and 15 wt% PVAc) the tan δ peaks of PVAc phase are located at lower temperatures than the corresponding to neat PVAc. In samples with nodular morphology tension stresses around the PVAc small particles arise due to the differences in expansion coefficient between epoxy thermoset and PVAc; these stresses contribute to decrease the T_g of PVAc, like it occurs in rubber-modified epoxies [20]. This effect could explain the gradual increase in the PVAc tan δ peak temperature with the PVAc content, because as the PVAc content increases the morphology gradually changes from nodular to combined until the total inversion is achieved, where this effect is not present (Table 2). To explain the lowering of the T_g of the thermoplastic phase in modified epoxy thermosets, it has been frequently argued that epoxy oligomers could have been dragged in the thermoplastic-rich phase producing a plasticizer effect. However the similar PVAc T_g obtained in samples with inverted morphologies and neat PVAc suggests that this effect is unlikely in PVAc/epoxy thermosets.

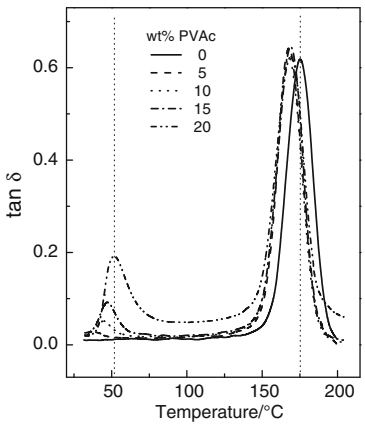

Fig. 4 tan δ-temperature isochrones (1 Hz) for PVAc/epoxy thermosets with different PVAc contents. Vertical lines indicate the maxima in tan δ for neat polymers: PVAc and epoxy

Table 2 DMTA results: tan δ peaks at 1 Hz for samples containing different content of PVAc and DSC results: T_g from scans at 10 °C min^{-1}

PVAc/wt%	T_{peak}/°C		T_g/°C	
	PVAc-phase	Epoxy-phase	PVAc-phase	Epoxy-phase
0	–	175	–	159
5	39	168	37	154
10	44	167	39	154
15	47	169	40	154
20	52	169	44	153
25	52	170	–	–
100	52	–	44	–

For all the compositions studied the α-relaxation peak of the epoxy-rich phase is located at lower temperature than in neat epoxy (Table 2). All the samples are totally cured as it was confirmed by DSC, showing the DSC scan no residual exotherm. Thus, the displacement of the epoxy α-relaxation peaks may reflect that some PVAc remains mixed in the epoxy phase. The Fox rule [21] for miscible blends was applied to predict the composition of epoxy rich phase

$$\frac{1}{T_g} = \frac{w_1}{T_{g1}} + \frac{1 - w_1}{T_{g2}} \quad (2)$$

where the subscripts 1 and 2 refer to epoxy and PVAc, respectively, and w is the weight fraction of the blend having glass transition T_g. Using the data in Table 2, a composition of ~4 wt% PVAc was calculated for the epoxy-rich phases independently of the overall blend composition. The height of tan δ peaks is an indication of the damping characteristic of the material, as it was expected by increasing the content of PVAc in the blend the height of its α-relaxation increases (Fig. 4). However, the heights of the epoxy α-relaxation do not decrease as the epoxy content lowers instead when the PVAc is present the tan δ peaks become higher than in neat epoxy thermoset. As it was discussed above in the blends, the epoxy phase has a ~4 wt% PVAc which would improve the damping of the epoxy α-relaxation.

Figure 5 shows the loss modulus–temperature profiles for samples with different PVAc contents, the curves show two maxima related with the PVAc-rich phase and with the epoxy-rich phase relaxations. The shape and size of E''–temperature curves give information about the sample morphology. Thus, for blends with nodular morphology the height of the E'' peak corresponding to PVAc phase is lower

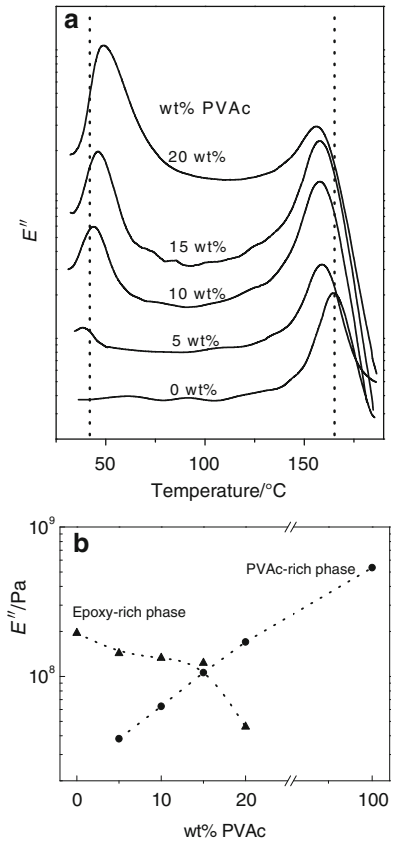

Fig. 5 **a** Loss modulus–temperature profiles at 1 Hz for PVAc/epoxy thermosets with different PVAc content. (The curves were displaced vertically for clarity). **b** Maximum intensity of loss modulus versus PVAc content for PVAc-rich phase (●) and for epoxy-rich phase (▲) in PVAc/epoxy thermosets

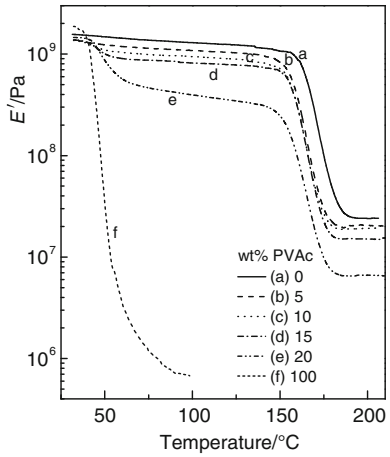

Fig. 6 Storage modulus (E')–temperature isochrones (1 Hz) for PVAc/epoxy thermosets with different PVAc contents: *a* neat epoxy, *b* 5 wt%, *c* 10 wt%, *d* 15 wt%, *e* 20 wt%, and *f* neat PVAc

than the height of E'' peak associated to the epoxy phase, but for blends containing 15 wt% of PVAc the heights of both E'' peaks are similar indicating that a change in the morphology is taking place. Figure 5b illustrates the variation of E'' heights with the composition for both relaxations; the total inversion would correspond to composition beyond the crossing of the lines (15 wt% PVAc).

The storage modulus (E')–temperature isochrones for samples with different PVAc content are shown in Fig. 6. In the glassy state, i.e. below the T_g of PVAc, E' varies with the PVAc content in a similar way than the tensile modulus (Table 1). Usually, the E' modulus determined by DMTA is lower than Young's modulus from tensile tests, this is due to the small size of the DMTA specimens that conduces to an effective length higher than the length between clamps [22, 23], thus the E' modulus of the samples at 30 °C are lower than the tensile modulus at room temperature and this difference would not only be due to the difference in temperature. As it was expected E' decreases as the temperature increases, a drop in E' appears at temperatures close to the PVAc T_g, being more important as the PVAc content raises.

Beyond the T_g of PVAc, the samples maintain the modulus value up to ~150 °C, where E' drops two decades as result of entering in the glass transition zone of the epoxy network. The morphology has a great influence on the variation of E' with temperature being the drop more important for inverted morphologies. Figure 7 illustrates the E'-composition dependence at 80 °C, similar behaviour is displayed for temperatures between 60 and 100 °C.

Several models have been developed in order to correlate the modulus of a biphasic material with its composition and morphology. The simplest expressions to predict the elastic properties of a two-phase polymer blend are the rule of mixtures

$$E' = \phi_1 E'_1 + \phi_2 E'_2 \tag{3}$$

and the inverse rule of mixtures

$$\frac{1}{E'} = \frac{\phi_1}{E'_1} + \frac{\phi_2}{E'_2} \tag{4}$$

being E', E'_1 and E'_2 the modulus of the composite and of each component and ϕ_1 and ϕ_2 their volume fractions. These equations give the upper and lower bounds for the E'-composition dependence as it is shown in Fig. 7 in which weight fractions were taken instead of the volume fractions.

The Kerner equation was proposed to predict the modulus of materials formed by spherical particles dispersed in a continuous matrix [24]

$$E' = E'_1 \frac{\frac{\phi_2 E'_2}{(7-5\nu_1)E'_1+(8-10\nu_1)E'_2} + \frac{\phi_1}{15(1-\nu_1)}}{\frac{\phi_2 E'_1}{(7-5\nu_1)E'_1+(8-10\nu_1)E'_2} + \frac{\phi_1}{15(1-\nu_1)}} \tag{5}$$

where ν_1 is Poisson's ratio for the matrix and subscripts 1 and 2 refer to the matrix and the dispersed phase, respectively.

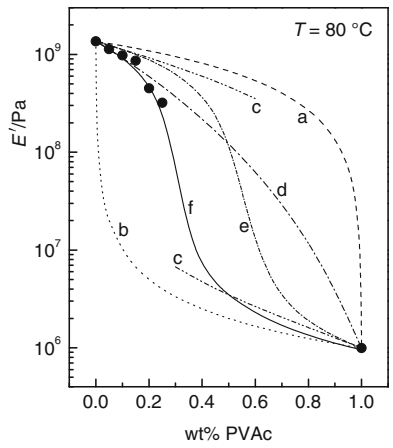

Fig. 7 E' data versus composition: experimental data at 80 °C (●) and modulus-composition models: *a* rule of mixtures, *b* inverse rule of mixtures, *c* upper and lower bounds of Kerner equation, *d* Davies equation, *e* Budiansky equation and *f* Budiansky equation with $\varepsilon = 0.69$

To calculate E' in systems in which both components are present as continuous phases, Davies proposed the equation [25]:

$$E'^{1/5} = \phi_1 E_1'^{1/5} + \phi_2 E_2'^{1/5} \tag{6}$$

The Budiansky model assumes that both components are continuous but the material is macroscopically homogeneous, and predicts the phase inversion in the mid composition range [26]. The E' is obtained by solving the equation

$$\frac{\phi_1}{1+\varepsilon\left(\frac{E_1'}{E'}-1\right)} + \frac{\phi_2}{1+\varepsilon\left(\frac{E_2'}{E'}-1\right)} = 1 \tag{7}$$

ε is related to Poisson's ratio, v, through the equation

$$\varepsilon = \frac{2(4-5v)}{15(1-v)} \tag{8}$$

for the blends v is calculated using a linear rule of mixtures, with $v = 0.5$ for PVAc in the rubbery state and $v = 0.35$ for the epoxy glass [27].

Equations 5–7 have been proposed for the shear modulus (G), in general the conversion from the shear-to-tensile modulus can be done by $E = 2G(1 + v)$, but it has been discussed [28, 29] that the error that is introduced using E instead of G is small. We have used these models to predict the experimental data in the range of temperatures 60–100 °C, where the PVAc is in the rubbery state and the epoxy is in the glassy state. This temperature range is away from the T_g's of the neat components, thus in that range their storage modulus are less temperature dependent. The calculated E' values at 80 °C by Eqs. 5–7 are shown in Fig. 7, similar behaviour is displayed for the other temperatures between 60 and 100 °C.

The samples with nodular morphology (5 wt% PVAc) and with combined morphology (10 and 15 wt% PVAc) show E' values between those calculated through Kerner or Budiansky and Davies equations. However, the E' values for the samples having inverted morphologies (20 and 25 wt% of PVAc) does not fit any of the models. Indeed, it can be seen a gap in E' when the inversion in morphology is completed, that is between 15 and 20 wt% PVAc. It may be readily observed from Fig. 7 that the Budiansky model shows a similar profile in the E'–composition curve than the experimental data, but it is shifted to higher compositions, i.e. the model predicts an inversion around 55 wt% of PVAc and overestimates the modulus of inverted morphologies, this fact has been frequently reported [9, 28–30]. Based on this observation and knowing that the inversion in the Budiansky equation is very dependent on the ε value, it was applied taking ε as a fitting parameter. The best fit was obtained for $\varepsilon = 0.69$ (Fig. 7). According to Eq. 10 a value of $\varepsilon = 0.69$ corresponds to $v = 6.7$, obviously this is an anomalous result. We have also studied the E'-composition in (polybenzyl methacrylate)/epoxy thermosets [9] and similar conclusions were reached, the values of ε that conduces to the best fit in that case was $\varepsilon = 0.74$ that corresponds to $v = 2.7$. In the Budiansky model, the inversion depends on the modulus and Poisson ratios of the two components, but in the thermodynamic analysis the main factor controlling the phase separation is the combinatorial contribution [1]. Accordingly, taking ε in the Budiansky model as a fitting parameter implies that it would include not only mechanical but also thermodynamic contributions.

Figure 8 shows the tan δ-temperature scans from −100 to 20 °C for PVAc/epoxy thermosets. The β-relaxation of the epoxy thermoset is centred around −55 °C and it is distributed over ~100 °C. This relaxation, observed in all epoxy–amine networks, is attributed to the motions of the hydroxylpropylether units (–CH_2–CH(OH)–CH_2–O–) [10].

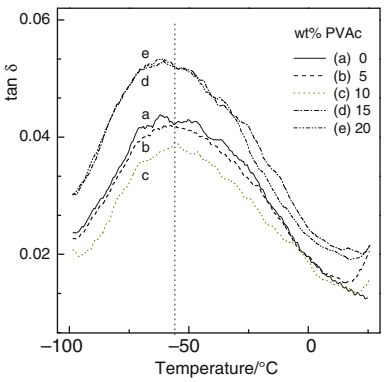

Fig. 8 tan δ-temperature isochrones (1 Hz) for PVAc/epoxy thermosets with different PVAc content and neat epoxy thermoset. Low-temperature scans

It is characterized by a broad mechanical relaxation peak: the low-temperature part should involve isolated movements, whereas the high-temperature part should correspond to short-range cooperative motions [10]. The presence of PVAc does not result in significant changes in the β-transition of the glassy epoxy phase. Only 15 and 20 wt% PVAc samples show slightly higher intensity of the β-relaxation being displaced to lower temperatures, likely due to residual PVAc that remains in the epoxy phase, interacting with the hydroxyls groups.

The frequency (f) dependence of the α and β relaxations, was also studied. Considering an Arrhenius dependence of the relaxations processes, the activation energy, can be estimated

$$E_a = -R\frac{d\ln f}{d\left(1/T_{max}\right)} \quad (9)$$

where E_a represents the activation energy for β-relaxations and the apparent activation energy for the α-relaxations, T_{max} is the temperature of the tan δ peak maximum at each frequency. Figure 9 shows log(frequency) versus ($1/T_{max}$) plots for the α-relaxations. In the range of frequencies studied (1–50 Hz) the Arrhenius plots for α and β relaxations are linear and from the slopes the activation energies were calculated according to Eq. 9. The values obtained were $E_a = 330 \pm 20$ and 620 ± 20 kJ mol^{-1} for the α-relaxation of PVAc and epoxy, respectively. The activation energy, E_a, characterizes the sensitivity of a relaxation process to temperature, which depends on the type of motions concerned. The difference in E_a values between PVAc and epoxy α-relaxations is related to the major flexibility of the PVAc chain compared to the highly crosslinked epoxy network at their respective T_gs. The E_a values obtained for the α-relaxations of PVAc and of epoxy in the blends do not show any significant variation with the thermoset composition, neither the E_a values obtained for the β-relaxation of the epoxy ($E_a = 63 \pm 4$ kJ mol^{-1}) varies with the composition. Therefore, the small amount of PVAc that remains mixed with the epoxy phase does not influence the sensitivity of epoxy network to temperature changes.

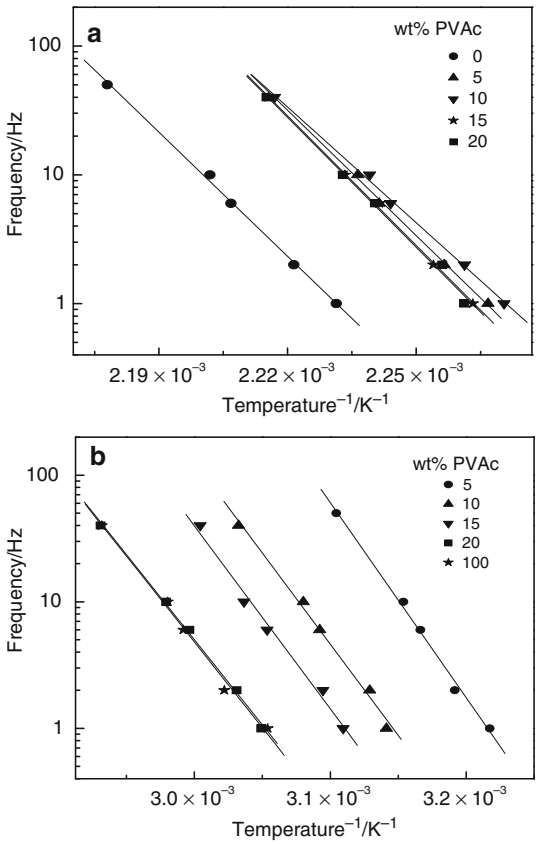

Fig. 9 Arrhenius plots for the dynamic mechanical α-relaxation of **a** epoxy and **b** PVAc in PVAc/epoxy thermosets

Conclusions

PVAc/epoxy thermosets are phase separated, arising two phases that correspond to a PVAc-rich phase and to the epoxy rich-phase. The morphology evolves from nodular to inverted as the PVAc content increases. Intermediate compositions (10–15 wt% of PVAc) present combined morphologies, in which nodular and inverted regions are detected.

The fracture surfaces of the blends show less brittle behaviour than neat epoxy thermoset. The tensile properties at room temperature indicate that the combined morphologies present the most ductile behaviour, in agreement with the data of fracture toughness previously reported. In the samples with inverted morphology the thermoplastic determines the fracture behaviour. There are evidences of good interfacial interactions between PVAc and epoxy, both in combined and inverted morphologies.

The detection of two T_gs (two α-relaxations) is consistent with biphasic morphology. The blends that present regions with nodular morphology show PVAc T_gs lower than the one of neat PVAc, which is attributed to the state of stresses around PVAc particles. The T_g of the epoxy is lower in the blends than in neat epoxy thermosets which is related to the presence of small amounts of PVAc in epoxy phase.

The profile of E''–temperature curves is correlated with the change in morphology that occurs as the PVAc content increases. The E'–temperature curves are highly dependent on the morphology and a significant drop in E' is detected when the morphology becomes inverted.

E'-composition dependence is predicted using several models for two-phase composites: samples with nodular and combined morphologies show moduli in between

Kerner or Budiansky and Davies models, but E' values for samples with inverted morphology do not fit any model. Budiansky equation overestimates the E' values and the inversion composition. A good prediction is obtained taking ε in the Budiansky equation as a fitting parameter.

Small changes of epoxy β-relaxations appear in the PVAc/epoxy thermosets which are attributed to the small amount of PVAc that remains in the epoxy phase, interacting with the hydroxyl groups of the epoxy thermoset.

The apparent E_a values of PVAc and epoxy α-relaxations and the E_a values of the epoxy β-relaxation do not show significant variation with the blend composition.

Acknowledgements Financial support for this study by CAM (S-0505/MAT0227 Interfaces Project) and by MEC (MAT 2006-02123) is acknowledged.

References

1. Pascault JP, Williams RJJ. Formulation and characterization of thermoset-thermoplastic blends. In: Paul DR, Bucknall CB, editors. Polymer blends. New York: Wiley; 2000. p. 379–415.
2. Johnsen BB, Kinloch AJ, Taylor AC. Toughness of syndiotactic polystyrene/epoxy polymer blends: microstructure and toughening mechanisms. Polymer. 2005;46:7352–69.
3. Thomas R, Durix S, Sinturel C, Omonov T, Goossens S, Groeninckx G, Moldenaers P, Thomas S. Cure kinetics, morphology and miscibility of modified DGEBA-based epoxy resin—effects of liquid rubber inclusion. Polymer. 2007;48:1695–710.
4. Peña G, Eceiza A, Valea A, Remiro P, Oyanguren P, Mondragón I. Control of morphologies and mechanical properties of thermoplastics-modified epoxy matrices by addition of a second thermoplastic. Polym Int. 2003;52:1444–53.
5. López J, Rico M, Montero B, Díez J, Ramirez C. Polymer blends based on an epoxy-amine thermoset and a thermoplastic. Effect of thermoplastic on cure reaction and thermal stability of the system. J Therm Anal Calorim. 2009;95:369–76.
6. López J, Rico M, Ramirez C, Montero B. Epoxy resin modified with a thermoplastic. Influence of modifier and reaction temperature on the phase separation. J Therm Anal Calorim. 2009. doi: 10.2007/s10973-009-0441-5.
7. Mondragón I, Remiro M, Martin MD, Valea A, Franco M, Bellenguer V. Viscoelastic behaviour of epoxy resins modified with poly(methyl methacrylate). Polym Int. 1998;47:152–8.
8. Prolongo SG, Salazar A, Ureña A, Rodríguez J. Effect of hydroxyls content on the morphology and properties of epoxy/poly(styrene-co-allyalcohol) blends. Polym Eng Sci. 2007;47:1580–7.
9. Prolongo MG, Arribas C, Salom C, Masegosa RM, Dynamic mechanical properties and morphology of poly(benzyl methacrylate) modified epoxy thermoset. Polym Eng Sci. 2009. doi:10.1002/pen.21707.
10. Heux L, Halary JL, Lauprêtre F, Monnerie L. Dynamic mechanical and ^{13}C n.m.r. investigations of molecular motions involved in the β relaxation of epoxy networks based on DGEBA and aliphatic amines. Polymer. 1997;38:1767–78.
11. Sivanlingam G, Karthik R, Madras G. Blends of poly(ε-caprolactone) and vinyl acetate: mechanical properties and thermal degradation. Polym Degrad Stabl. 2004;84:34551.
12. Lapprand A, Arribas C, Salom C, Masegosa RM, Prolongo MG. Epoxy resins modified with poly(vinyl acetate). J Mater Process Technol. 2003;143–144:827–31.
13. Sánchez-Cabezudo M, Prolongo MG, Salom C, Masegosa RM. Cure kinetics of epoxy resin and thermoplastic polymer. J Therm Anal Calorim. 2006;86:699–705.
14. Arribas C, Sepúlveda L, Salom C, Masegosa RM, Prolongo MG. Morphology effect on the hydrothermal ageing of a thermoplastic modified epoxy thermoset. Polym Eng Sci. 2007;47:960–8.
15. Prolongo MG, Arribas C, Salom C, Masegosa RM. Phase separation, cure kinetics and morphology in epoxy/poly(vinyl acetate blends). J Appl Polym Sci. 2007;103:1507–16.
16. Zheng S, Hu Y, Guo Q, Wei J. Miscibility, morphology and fracture toughness of epoxy/poly(vinyl acetate) blends. Colloid Polym Sci. 1996;274:410–7.
17. Oyanguren PA, Galante MJ, Andromaque, Frontini PM, Williams RJJ. Development of bicontinuous morphologies in polysulfone-epoxy blends. Polymer. 1999;40:5249–55.
18. Chikhi N, Fellahi S, Bakar M. Modification of epoxy resin using reactive liquid (ATBN) rubber. Eur Polym J. 2002;38:251–64.
19. Montserrat S, Calventus Y, Hutchinson JM. Effect of cooling rate and frequency on the calorimetric measurement of the glass transition. Polymer. 2005;46:12181–9.
20. Verchere D, Pascault JP, Sautereau H, Moschiar SM, Ricardi CC, Williams RJJ. Rubber-modified epoxies. II. Influence of cure schedule and rubber concentration on the generated morphology. J Appl Polym Sci. 1991;42:701–16.
21. Fox TG. Influence of diluent and of copolymer composition on the glass temperature of a polymer system. Bull Am Phys Soc. 1956;1:123.
22. Riande E, Díaz-Calleja R, Prolongo MG, Masegosa RM, Salom C. Polymer viscoelasticity: stress and strain in practice. New York: Marcel Dekker; 2000. p. 283–5.
23. Deng S, Hou M, Ye L. Temperature dependent elastic moduli of epoxies measured by DMA and their correlations to mechanical testing data. Polym Test. 2007;26:803–13.
24. Kerner EH. The elastic and thermo-elastic properties of composite media. Proc Phys Soc Lond B. 1956;69:808–13.
25. Davies WEA. The elastic constant of a two-phase composite material. J Phys D Appl Phys. 1971;4:1176–81.
26. Budiansky B. On the elastic moduli of some heterogeneous materials. J Mech Phys Solids. 1965;13:223–7.
27. Johnsen BB, Kinloch AJ, Mohammed RD, Taylor AC, Springer S. Toughening mechanism of nanoparticle-modified epoxy polymers. Polymer. 2007;48:530–41.
28. Hourston DJ, Schäfer F, Gradwell MHS, Song M. TMXDI-based poly(etherurethane)/polystyrene interpenetrating polymer networks 2.T_g behaviour, mechanical properties and modulus-composition studies. Polymer. 1998;39:5609–17.
29. Ryan AJ, Stanford JL, Still RH. Thermal, mechanical and fracture properties of reaction injection-moulded poly(urethane-urea)s. Polymer. 1991;32:1426–39.
30. Hourston DJ, Schäfer F. Poly(ether urethane)/poly(ethyl methacrylate) interpenetrating polymer networks: morphology, phase continuity and mechanical properties as a function of composition. Polymer. 1996;37:3521–30.